



A Video Plankton Recorder user guide: Lessons learned from in situ plankton imaging in shallow and turbid coastal waters in the Belgian part of the North Sea

Anouk Ollevier^{a,*}, Jonas Mortelmans^a, Michiel B. Vandegehuchte^a, Roeland Develter^a, Marleen De Troch^b, Klaas Deneudt^a

^a Flanders Marine Institute (VLIZ), Wandelaarkaai 7, 8400 Ostend, Belgium

^b Biology Department, Marine Biology Research group, Ghent University, Krijgslaan 281-S8, 9000 Gent, Belgium

ARTICLE INFO

Keywords:

Zooplankton
In situ imaging
Plankton distribution
Turbidity

ABSTRACT

Optical imaging devices such as the Video Plankton Recorder (VPR) harness unique capabilities to perform in situ observations and observe planktonic organisms in their natural environmental context. However, applying this technology in shallow and turbid coastal waters comes with a number of challenges. Depending on the research goal, methodological choices need to be made regarding the appropriate towing procedure and instrument settings, like magnification or field of view. In addition, limitations can be expected related to the physical characteristics of the water column, more specifically regarding suspended matter concentration and turbidity. To inform VPR users on the possibilities and limitations of the device in shallow and turbid coastal waters, this paper evaluates a number of specific deployment procedures in the Belgian part of the North Sea (BPNS). For three different towing procedures the practical feasibility, characteristics and output are assessed and the assets and liabilities for each of the tow types are discussed. A Z-shaped and a clover-shaped tow type are seen as best fit for detailed characterization of the plankton community of a limited geographical area. A straight tow type is more suitable for plankton studies over a larger area, with the potential to capture local plankton abundance peaks and to determine the relation with the spatial variation of the environmental conditions. The capacity of the various VPR magnification settings to capture specific plankton taxa or size groups, was tested during four straight line transects with different magnifications. The highest magnification can be used for organisms from 0.3 to 0.7 mm while the low magnification allows to observe larger organisms within the size range of 1.0 to 3.8 mm. Finally, the boundary conditions for the deployment of the VPR related to the turbidity of the water column were defined and the implications for deployment within the study area were investigated. This study shows that high turbidity values over 6.2 NTU inhibit the collection of useable data, complicating the VPR's application in many coastal and transitional waters.

1. Introduction

Zooplankton are a significant component of the marine ecosystem (Castellani and Edwards, 2017), as they play a pivotal role in biogeochemical cycles (Steinberg and Landry, 2017), and form a crucial link between phytoplankton and higher trophic levels, to which e.g., economically important fish species belong (Nielsen et al., 1993). Most zooplankton species are short-living, have a fast generation time and are sensitive to temperature fluctuations (Mackas et al., 2012; Chivers et al., 2017). With climate change, rising sea temperatures and ocean

acidification, their characteristics make them highly suitable organisms to evaluate the effects of anthropogenic influences on ecosystem functioning.

Typically, plankton research starts from physical samples collected by means of vertical hauls (e.g., Castellani and Edwards, 2017) followed by time-consuming species identification and estimation of zooplankton abundances at the species level under a light microscope. As a result of this labor-intensive work, this methodology is restricted to a limited spatio-temporal coverage. It is not able to grasp large-scale distribution patterns of the plankton community, such as the vertical distribution

* Corresponding author.

E-mail address: anouk.ollevier@vliz.be (A. Ollevier).

<https://doi.org/10.1016/j.seares.2022.102257>

Received 29 March 2022; Received in revised form 3 August 2022; Accepted 5 August 2022

Available online 9 August 2022

1385-1101/© 2022 The Authors. Published by Elsevier B.V. This is an open access article under the CC BY-NC-ND license (<http://creativecommons.org/licenses/by-nc-nd/4.0/>).

(Jacobsen and Norrbin, 2009) or small-scale patchiness of species and communities (Gallienne et al., 2001; Ashjian et al., 2001). Additionally, it misses information on fragile particles such as detritus and gelatinous plankton (Remsen et al., 2004), as these can be damaged or destroyed during the sampling process.

To counter the problems of physical sampling, in situ imaging tools have been developed and are frequently used for plankton research. An example of such a device is the Video Plankton Recorder (VPR). It is essentially an underwater microscope that captures in situ photographs of plankton and marine particles in the size range of 100 μm up to a few centimeters. It has the advantage to observe marine diversity without damaging it, and the simultaneous abiotic, spatial and geographic measurements allow visualization of marine communities in 3D and research of their affinities with water quality parameters (Gallienne et al., 2001), vertical stratification (Pan et al., 2018; Jacobsen and Norrbin, 2009) or interactions with detritus and marine snow (Möller et al., 2012). It has proven to be a successful device for research strategies that aim to document the vertical distribution of organisms through the water column or where high spatial and temporal resolution is necessary, which cannot be achieved with traditional sampling methods (Gallienne et al., 2001; Pan et al., 2018; Jacobsen and Norrbin, 2009; Ashjian et al., 2001).

A review of the literature showed that various towing procedures have been used for the deployment of a VPR (Sainmont et al., 2014; Gislason et al., 2016; Möller et al., 2012; Davis et al., 2004). During deployment of the VPR, a dedicated winch is used to tow the device behind the research vessel. Depth of the VPR (by reeling the winch cable in or out), the speed of winching (by reeling the winch faster or slower), the magnification of the camera, the user-defined parameters in the AutoDeck software and the sail trajectory are chosen by the scientist. These decisions result in different sampling methods and for each research question a specific strategy and customized towing procedure can be used. Few VPR studies substantiated their choices for the used tow types and up to our knowledge, no comparative studies on the deployment methods of the VPR have been published so far.

This paper aims to allow future VPR users to make a well-considered choice on VPR deployment method and application, based on the research purpose. We evaluate three types of towing the VPR in a continuous way and four magnification settings. Secondly, the technical limitations of the VPR related to turbidity are investigated. This will inform us in which water conditions the VPR can be deployed and will enable us to discern the turbidity threshold for images to allow plankton analysis.

2. Materials and methods

2.1. Study area

The Belgian part of the North Sea (BPNS) is a relatively shallow area (up to 40 m) with several subtidal sandbanks (Vanaverbeke et al., 2000). The water column is well-mixed and characterized by a high nutrient concentration (De Galan et al., 2004) due to the outflow from the rivers IJzer, Scheldt and Maas (Nihoul et al., 1978). Especially the Scheldt has a dominant influence in terms of SPM, forming a high turbidity zone near the coast (Fettweis et al., 2007).

Three cruises (Fig. 1) with the RV Simon Stevin were performed to study the tow types, magnification settings and turbidity limit of the VPR. For the tow type cruise (May 2020) and magnification setting cruise (June 2020) a region with a low SPM concentration was selected where turbidity was not expected to pose a problem for the effective use of the VPR. To find the turbidity limit of the VPR (June 2020), a location near the mouth of the Scheldt was chosen. This region is, based on previous experience in the study area, known to hamper the collection of images with the VPR due to relatively high concentrations of SPM and low visibility of the water column. The turbidity gradient with lower turbidity values in the areas away from the Scheldt allows to determine the turbidity limit of the VPR. Depending on the functioning of the VPR at this start point, the vessel would sail away from or towards the coast, heading towards clearer or more turbid conditions, respectively.

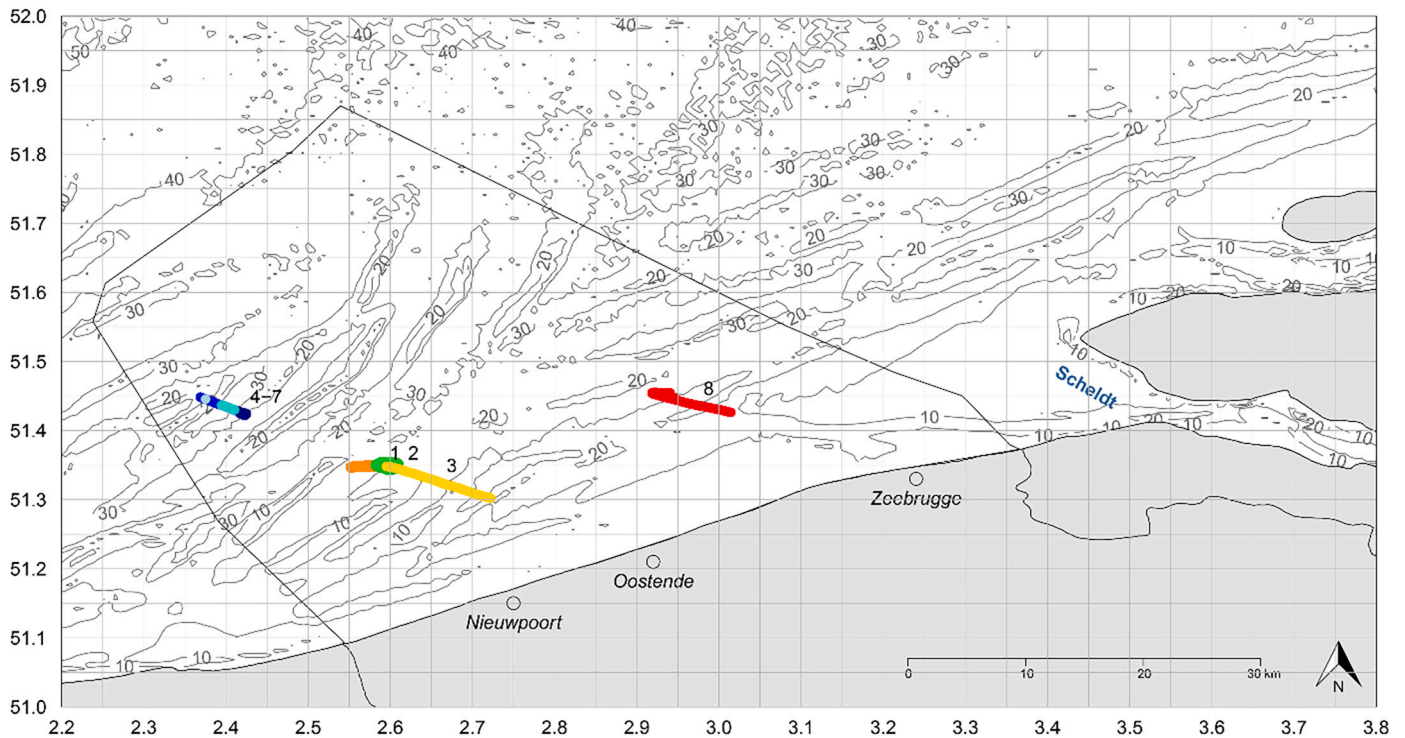


Fig. 1. Map of the Belgian part of the North Sea, with indication of the trajectories. The tow type cruise with in orange (1) the Z-shaped pattern, in green (2) the clover pattern and in yellow (3) the straight pattern. The magnification setting cruise with (4–7) magnification setting S0, S1, S2 and S3. The turbidity cruise (8). In addition to the numbers, each trajectory was also represented with a different color for clarity because some trajectories are positioned close to each other.

2.2. Video Plankton Recorder

The Video Plankton Recorder (Seascan, Inc.) is an optical underwater instrument for the in situ observation of plankton specimens and marine particles ranging in size from 100 μm up to a few centimeters. In this study a Real Time Video Plankton Recorder (Seascan, Inc.) allows for a real-time view of the observed particles on board of the vessel. A VPR makes use of dark field illumination, whereby the light sent out by the stroboscope is diffracted by particles of interest into the camera lens. The 1380 by 1034 pixel-sized images of the Real Time VPR are captured

$$\text{Density [ind/m}^3\text{]} = (\text{Number of individuals [ind]}/\text{Sampled volume [mL]}) * 1,000,000 \text{ [mL/m}^3\text{]} \quad (2)$$

by the 1.4 MegaPixel color camera at 25 frames per second. The Real Time VPR used in this study has arms that are located 590.8 mm away from each other on which the stroboscope and camera are mounted. It is equipped with an SBE 49 CTD (Sea-Bird Electronics, Inc.) and ECO Puck FLNTU fluorometer and turbidity sensor (WETLabs) to simultaneously collect hydrographic and environmental data. Image and sensor data of a Real Time VPR is transferred in real-time over a single mode fiber optic cable and captured by the AutoDeck software (Seascan, Inc.). Based on selected parameters (e.g., segmentation threshold, focus) plankton and other particle images are extracted from each image frame as regions of interest (ROIs) and saved to the computer's hard drive as TIFF files. Each ROI is tagged using a timestamp to allow synchronization with the hydrographic parameters that were stored in a separate logfile. All the image data were manually classified by sorting the zooplankton into the following categories: Amphipoda, Annelida, Appendicularia, Brachyura zoea, Calanoida, Caridea, Cnidaria, Ctenophora, Cumacea, Echinodermata, Harpacticoida and Pisces larvae. Other particles were classified as Appendicularia house, *Noctiluca*, *Phaeocystis*, detritus, bubbles, fibres, or unknown. All image and corresponding sensor data were subsequently stored in a MongoDB database that was consulted using the Studio 3 T graphical user interface (Studio 3T Team, 2022).

During deployment of a Real Time VPR, the scientist has to select the Real Time VPR's magnification setting and the parameters in the AutoDeck software. A Real Time VPR has four preset motor positions that determine the field of view, being $8.8 \times 6.6 \text{ mm}$, $20.8 \times 15.2 \text{ mm}$, $33.8 \times 25.5 \text{ mm}$, $46.5 \times 34.5 \text{ mm}$ in the Real Time VPR used in this study (Seascan, 2014). These correspond to magnification settings ranging from S0 to S3, which are the most zoomed in and zoomed out settings, respectively. The user-defined parameters in AutoDeck are segmentation threshold – low, segmentation threshold – high, focus – sobel, focus – std. dev, growth scale (%), minimum blob size (area) and minimum join distance. With the first four of these user-defined parameters in AutoDeck and the magnification setting, the CalDeck software (Seascan, Inc.) calculates the volume of water in focus per frame, to which will be referred as the imaged volume (per frame) in the remainder of the text.

With the imaged volume, one can calculate how much water was sampled by the VPR during a trajectory, the so called sampled volume. To calculate the sampled volume (formula 1) the imaged volume is multiplied by the number of frames per second (for the Real Time VPR

this is 25 fps) and the duration of data collection by the VPR. In this study, densities are based on the entire trajectory but densities can also be calculated for a specific part of a trajectory. In the latter case, a shorter deployment time with the respective number of plankton observed within that part of the trajectory should then be used in formula 1 and 2.

After validation of the ROIs, the plankton density [ind/m^3] per taxa of a VPR transect can be determined as:

In formula 2 there is a multiplication with 1,000,000 to convert the unit ind/mL to ind/m^3 .

2.3. Tow types

Three tow types were tested (Fig. 2). They were performed immediately after each other and have a starting point in the same area. The first tow type is a Z-shape, whereby the research vessel sails back and forth on a straight line. Each time the vessel turns, the VPR is deployed at a different depth, eventually resulting in a zigzag or Z-shaped pattern as viewed from the side of the water column. The trajectory is divided into three parts where the VPR was deployed at 24, 12 and 5 m depth, respectively. The VPR was used for approximately 30 min at each depth. The second tow type is undulating the VPR while sailing a clover-shaped pattern. Here the winch cable is reeled in and out at a speed of 0.05 m/s, in order to allow the VPR to move up and down through the water column. Seen from above, the vessel sails in the shape of a three-leafed clover, whereby each loop takes around 30 min. The third type is obtained by sailing a straight line whereby the VPR is undulating with a winch speed of 0.05 m/s. Hereafter, these tow types will be referred to as a 'Z-shaped', 'clover-shaped' and 'straight' pattern. The duration of each tow type was 1h43min, 1h27min and 1h38min for the Z-shaped, clover-shaped and straight pattern, respectively. A distance of 10.2, 10.2 and 8.3 km was covered by the Z-shaped, clover and straight pattern, respectively. For the Z-pattern, the vessel sailed back and forth on the same transect, meaning there is information for the three depths of the water column only for a 3.4 km long transect. During all transects, the vessel and VPR maintained a constant speed of 3–4 knots relative to the water column, independent of the current speed and direction.

For each tow type, the imaged volume of a VPR frame was 17.821 mL. This was based on magnification setting S1, a segmentation threshold – low of 0, a segmentation threshold – high of 135, a focus – sobel of 34 and a focus – std. dev 1 in AutoDeck. For the different tow types the AutoDeck parameters were kept the same to not introduce additional variance. The three tow patterns were compared to each other based on feasibility, biological data and abiotic data. In RStudio (version 1.4.1106; RStudio Team, 2020), biological and abiotic patterns were visually explored with 3D graphs (R package 'plot3D' and 'plot3Drgl') and evaluated by grouping data according to depth or location.

$$\text{Sampled volume [mL]} = \text{Imaged volume [mL/frame]} * 25 \text{ [frames/s]} * \text{Duration of VPR deployment [s]} \quad (1)$$

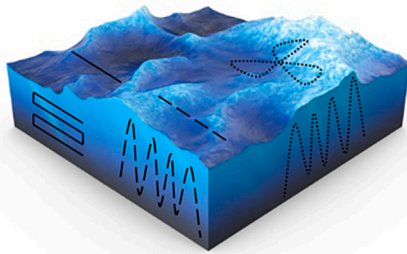


Fig. 2. Schematic representation of the three different tow types. Solid line: a Z-shape while sailing a straight line ('Z-shaped pattern'). Dashed line: undulating the VPR while sailing a straight line ('straight pattern'). Dotted line: undulating the VPR while sailing a clover-shaped pattern ('clover-shaped pattern').

2.4. Magnification settings

In June 2020, four VPR transects with different magnification settings were performed (Fig. 1). The imaged volume for the magnification setting S0, S1, S2 and S3 were 2.021 mL, 23.391 mL, 192.657 mL and 285.758 mL, respectively (formula 1). This was based on a segmentation threshold – low, segmentation threshold – high, focus – sobel and focus – std. dev of 0, 130, 15, 1 for S0; 0, 135, 25, 3 for S1 and S2; and 0, 155, 40, 5 for S3 in AutoDeck. The captured 1380 by 1034 pixel-sized VPR images had a size of 8.8×6.6 mm, 20.8×15.2 mm, 33.8×25.5 mm, 46.5×34.5 mm for magnification setting S0, S1, S2 and S3, respectively. Settings S1 till S3 were deployed for about one hour, S0 for approximately half an hour (S0: 23 min, S1: 64 min, S2: 71 min, S3: 59 min). The transect was performed as a straight line while undulating the VPR. To research the size range of the observed plankton by each magnification settings, length measurements were performed on the VPR images. Maximum 10 ROIs of each taxon at each magnification setting were manually measured in ImageJ. After setting the scale, measurements were made based on a straight line that spanned the extreme ends of an organism. The measurements thus are not the head-tail length but are the longest or widest part of an organism to estimate the range in which a given magnification setting can detect a particle. For species such as Annelida or Appendicularia that are sometimes curved or contorted on the image, the measurement is an underestimation of the actual head-to-tail length of the organism. The results were compared with a large set of ZooScan length measurements of a WP2 sample taken close to the transect that gives an estimation of the general size of the plankton community during that month. For this, zooplankton was sampled with a 200 μ m WP2 net which was deployed vertically and equipped with a flowmeter, following the protocol of Mortelmans et al. (2019). Zooplankton collected in the cod-end was sedated by soda water and fixated in a 4% formaldehyde solution. In the lab, the fixative was replaced by 70% ethanol. The sample was digitized by the ZooScan plankton imaging device and processed by ZooProcess and Plankton Identifier (PkID) in order to detect, measure and classify the digitized objects (Grosjean et al., 2004; Gorsky et al., 2010). Size estimations of the body length by the ZooScan were based on the major axis of the best fitting ellipse (Gorsky et al., 2010). It should be noted that fixation in formaldehyde causes shrinkage of specimens, in particular of soft-bodied organisms such as Appendicularia, Chaetognatha, Ctenophores and Cnidaria (Thibault-Botha and Bowen, 2004; Nishikawa and Terazaki, 1996; De Lafontaine and Leggett, 1989), causing length measurements from the ZooScan to be smaller compared to the ImageJ measurements from living organisms.

2.5. Turbidity

To assess the turbidity limitations of the VPR, a transect parallel to a

known turbidity gradient (SPM concentrations from Flanders Marine Institute, 2019) was followed (Fig. 1). By towing the VPR through different turbidity zones, the impact of turbidity on the operation of the VPR and the capturing of images was investigated. Turbidity measurements by the turbidity sensor on the VPR are expressed in mV and can be converted to NTU values with formula 3, where 0.069 is a value based on the calibration of the sensor.

$$\text{Turbidity [NTU]} = 200^* (\text{voltage of turbidity sensor [V]} - 0.069) \quad (3)$$

To assess turbidity for the whole BPNS, 17 stations were sampled for Suspended Particulate Matter (SPM) and Secchi depth, following the protocol described in Mortelmans et al. (2019). To determine the SPM concentrations, one liter of unfiltered seawater from the Niskin bottles, closed at 3 m depth, was taken and poured in a labeled recipient and stored at 4 °C. After the cruise the samples were processed by the Flanders Environment Agency. For the Secchi disk measurements, a 30 cm Secchi disk was lowered into the water column from the side of the vessel until it was no longer visible. It was subsequently hauled up and the depth at which it became visible was noted. Based on these data, interpolated maps ('sp' package) for the entire BPNS were made in RStudio. The location where the captured ROIs became blurry or unusable during the VPR trajectory, was subsequently plotted on these maps to determine at which SPM and Secchi values the VPR no longer functioned optimally.

3. Results

3.1. Tow types

3.1.1. Abiotic measurements

Temperature differences within a tow were observed (Fig. 3). For the Z and clover-shaped pattern, the temperature differed 0.2 and 0.3 °C between the bottom and surface layer. In the clover-shaped pattern the vertical temperature gradient was visible in every undulation. For the straight pattern (Fig. 3C) there were also vertical temperature differences, but the main temperature difference appeared horizontally between the beginning and end of the trajectory (difference of 0.7 °C). In the straight pattern, the end point was located the furthest away from the starting point (8.3 km) compared to the other tow patterns, so that the differences that existed over a larger area were observed.

For all tow types, a similar pattern was observed with higher turbidity values close to the sea bottom (Fig. 4). The majority of the observed turbidity values in the water column ranged between 0 and 4 NTU, although maximum turbidity values could reach to 10.2, 15.2, 19.0 NTU for a short period of time in the three patterns.

3.1.2. Biotic measurements

The densities of most plankton taxa were of the same order of magnitude for the different tow types (Table 1). Calanoida and Cnidaria were more abundant in the Z-pattern. In the clover pattern, higher *Phaeocystis* abundances and lower Echinodermata and *Noctiluca* abundances were observed compared to the other tow types. For the less abundant taxa it was noted that two taxa were not encountered in the clover pattern and that four taxa were absent in the Z-pattern. Despite the absence of certain taxa in the Z-pattern, it had the highest total summed abundance of species (17,576 ind/m³). For the clover and straight pattern, this was 16,952 and 16,100 ind/m³, respectively.

Community composition was calculated for each tow type as taxa proportional distributions (Table 1). In all tow types *Noctiluca* and *Phaeocystis* were the most abundant taxa, making up 73.62, 79.50 and 74.49% of the encountered organisms, in the Z, clover and straight pattern, respectively. These were followed by Calanoida, Echinodermata and Cnidaria, together contributing 22.93, 17.29 and 20.84% to the plankton community, respectively.

The three dimensional spatial distribution of the most abundant taxa

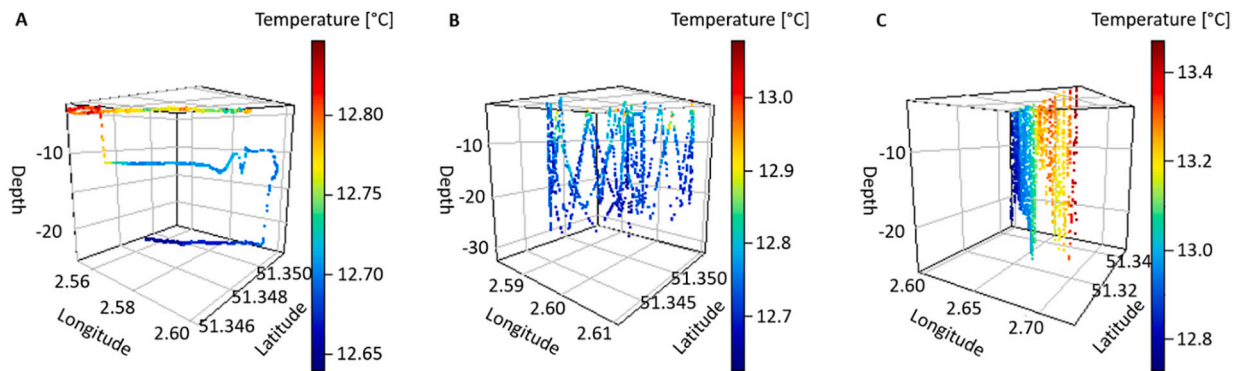


Fig. 3. Plots of the temperature [°C] for each tow type: (A) Z-pattern, (B) clover pattern and (C) straight pattern. Note the different scales on the axes: the straight pattern spans a much wider latitudinal range.

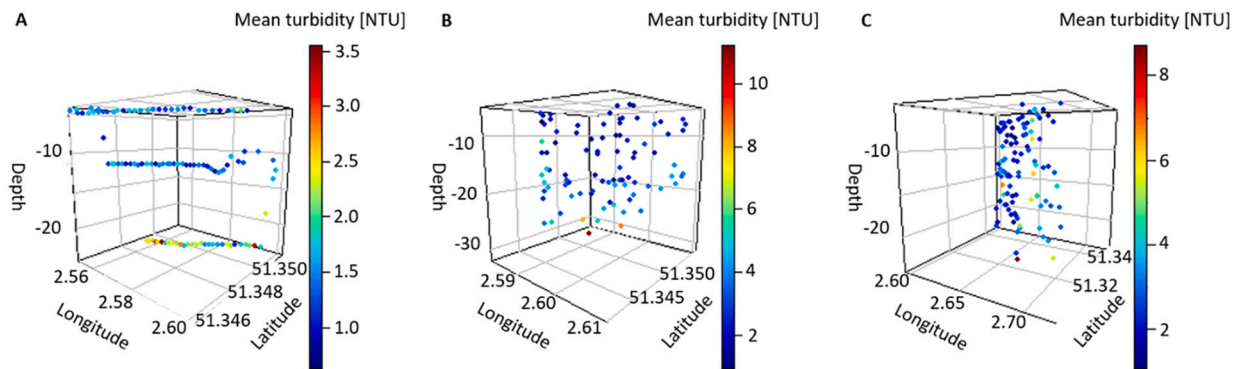


Fig. 4. Turbidity measurements [NTU] grouped and averaged per minute for each tow type: (A) Z-pattern, (B) clover pattern and (C) straight pattern. Note the different scales on the axes: the straight pattern spans a much wider latitudinal range.

Table 1

The absolute [ind/m³] and relative [%] plankton density per tow type.

Taxa	Absolute density [ind/m ³]			Relative density [%]		
	Z-shaped	Clover-shaped	Straight	Z-shaped	Clover-shaped	Straight
Amphipoda	0.00	21.46	9.50	0.00	0.13	0.06
Annelida	63.52	128.75	171.08	0.36	0.76	1.06
Appendicularia	453.70	268.23	351.66	2.58	1.58	2.18
Brachyura zoea	18.15	42.92	47.52	0.10	0.25	0.30
Calanoida	2050.72	1555.73	1435.15	11.67	9.18	8.91
Caridea	54.44	53.65	76.03	0.31	0.32	0.47
Cnidaria	653.33	375.52	437.20	3.72	2.22	2.72
Ctenophora	0.00	0.00	19.01	0.00	0.00	0.12
Cumacea	0.00	21.46	47.52	0.00	0.13	0.30
Echinodermata	1324.80	997.81	1482.68	7.54	5.89	9.21
Harpacticoida	0.00	10.73	19.01	0.00	0.06	0.12
Noctiluca	9518.62	7682.09	9086.14	54.16	45.31	56.43
Phaeocystis	3420.90	5793.75	2908.33	19.46	34.17	18.06
Pisces larvae	18.15	0.00	9.50	0.10	0.00	0.06
Σ	17,576.32	16,952.09	16,100.34	100	100	100

were analyzed. The most striking observations were the differences in the vertical distribution of *Noctiluca* and *Phaeocystis* in all tow types, and the differences in taxon abundance in the horizontal distribution of the straight pattern. For the Z-pattern, a segment of 20 min of data for each depth was selected from parts of the transect that overlapped as viewed from above. For the other tow types, plankton densities were grouped in three depth bins representing the surface, middle and deep layer to research its vertical patterns. In all tow types, *Noctiluca* was more abundant closer to the surface whereas *Phaeocystis* reached higher abundances closer to the sea floor. To illustrate, densities of these taxa are represented for the Z-pattern in Table 2 and show that *Noctiluca*

densities were 17,442 ind/m³ at the surface 3788 ind/m³ near the bottom whereas the densities of *Phaeocystis* were 1356 ind/m³ in the upper layers and 5752 ind/m³ in the deeper layers. The data of the straight pattern was divided in a part north and south of the Kwintebank, a sandbank in front of Nieuwpoort (Table 3). This separation showed that *Calanoida*, *Cnidaria* and *Phaeocystis* were more abundant north of the sandbank, with densities being 8, 1.2 and 4 times higher, respectively. *Noctiluca* however, was less abundant in the area north of the Kwintebank.

Table 2

Vertical distribution of *Noctiluca* and *Phaeocystis* in the Z-pattern. The surface layer included specimens from 4 to 6 m, the middle layer from 11 to 13 m and the deep layer from 23 to 24 m.

Taxa	Bin	Mean depth [m]	Count [ind]	Deployment time [s]	Density [ind/m ³]
<i>Noctiluca</i>	Surface	4.99	373	1200	17,441.97
	Middle	11.57	157	1200	7341.53
	Deep	24.17	81	1200	3787.67
<i>Phaeocystis</i>	Surface	4.99	29	1200	1356.08
	Middle	11.58	61	1200	2852.44
	Deep	24.17	123	1200	5751.64

Table 3

Horizontal distribution of the most abundant taxa in the straight pattern.

Taxa	Bin	Mean depth [m]	Count [ind]	Deployment time [s]	Density [ind/m ³]
Calanoida	North of sand bank	14.02	140	3642	2157.03
	South of sand bank	9.22	11	2259	273.24
Cnidaria	North of sand bank	13.89	31	3642	477.63
	South of sand bank	11.23	15	2259	372.60
<i>Noctiluca</i>	North of sand bank	12.02	493	3642	7595.82
	South of sand bank	9.50	463	2259	11,500.92
<i>Phaeocystis</i>	North of sand bank	13.72	266	3642	4098.36
	South of sand bank	11.69	40	2259	993.60

3.2. Magnification settings

3.2.1. The capture of images

More ROIs were saved with low magnification settings (S3) compared to high magnification settings (S0). Despite sampling only half so long as the other settings, S3 still captured more images than S0, S1 and S2 (Supplementary Material Table 3). Remarkable is the relatively high number of Appendicularia houses observed at magnification setting S3. With S3, also a higher number of plankton taxa was observed (11 taxa), while S0 on the other hand merely observed three plankton taxa. The densities of the majority of the plankton taxa are in the same order of magnitude along the different magnification settings. However, the density data of e.g., Calanoida and *Noctiluca* shows significant differences in abundance between the settings, with the highest abundances observed by the S0 magnification setting. The densities of this high magnification settings are often calculated based on just a few ROIs in the case of Calanoida and Cnidaria.

3.2.2. Information contained in the image data

The magnification and hence information contained in the images differs per magnification setting. More details were distinguishable with the high magnification setting (Table 5). Stomach content of *Noctiluca* cells was visible with S0, in contrast to S3 where a *Noctiluca* cell merely looks like a small sphere. In the latter, organisms appeared smaller with

a less pronounced shape and thus are harder to identify. However, despite the higher resolution of S0, it is not accurate enough to allow classification of organisms to species level. Furthermore, the majority of the S0 ROIs contained one particle, without overlap with any other plankton or detritus particle. For S1, S2 and S3, multiple particles were sometimes present on one image, which can give insight into how plankton interacts with the environment. It for example allows us to observe plankton feeding on detritus.

Cnidaria were observed at all magnification settings: at S0, S1 and S2 we mainly observed relative small Cnidaria, whereas in S3, another species of Cnidaria with a larger bell was observed which constituted a large part of the observed Cnidaria. Due to the large field of view, S3 is also suitable for observing larger species of jellyfish. Appendicularia and its gelatinous houses were not observed by the S0 magnification, but were detected abundantly by the S3 setting, meaning that they were commonly present in the water column (Supplementary Material Table 1). The larger size of Appendicularia and its gelatinous houses is therefore probably the reason why they were not detected by S0.

3.2.3. Length measurements

The mean size of the plankton taxa ranged from 0.350 mm to 0.859 mm in the WP2 net sample (Supplementary Material Table 1) and from 0.379 to 3.766 mm on the VPR images (Table 4). The larger organisms captured by the VPR (>2 mm) were Annelida, Appendicularia and its houses, Caridea, Cnidaria, Ctenophora, Cumacea, *Phaeocystis* colonies and Pisces larvae. Of those taxa, Appendicularia, Cnidaria and Cumacea were present in the WP2 sample, but with smaller mean sizes (0.803 mm, 0.859 mm and 0.847 mm, respectively) compared to the sizes observed at the different magnifications of the VPR (2.064–2.563 mm, 0.379–2.205 mm and 2.526 mm, respectively). Other taxa observed by both methods were Echinodermata and *Noctiluca*, which were one of the smaller taxa of the plankton community based on the length measurements of the WP2 sample. For the majority of the taxa imaged by the VPR, the mean size was larger in the lower magnification settings corresponding to the fact that the lower magnification settings are able to capture larger specimens. The mean size of taxa ranged between 0.379 and 0.715 mm for S0, 0.683 and 2.191 mm for S1, 0.694 and 3.069 mm for S2 and between 0.965 and 3.766 mm for S3.

3.3. Turbidity

3.3.1. Turbidity measurements

Turbidity data collected by the VPR shows a gradient with lower offshore turbidity values and high nearshore turbidity values with turbidity peaks up to 25.5 NTU. Simultaneous measurements on Secchi depth and SPM showed the same pattern with lower offshore turbidity values and high nearshore turbidity values (Fig. 5). Especially near the Scheldt Estuary low Secchi disk depths and high concentrations of SPM were observed.

3.3.2. Image data

When sailing through the turbidity zones, a distinction could be made based on the images captured by the AutoDeck software. In the areas further from the coast with a turbidity around 3.2 NTU good images were taken (Supplementary Material Table 2). The plankton particles were bright and contrasted against the dark background. In nearshore areas, a turbidity around 6.2 NTU yielded blurry images. The background on the images was much brighter, therefore making it harder to distinguish the particles of interest. When turbidity rose to 10.2 NTU, no images were recorded (Supplementary Material Table 2). The point when no more ROIs were stored corresponded approximately to a Secchi depth of 200 cm and a SPM concentration of 30 mg/L.

Table 4

Counts [ind], densities [ind/m³] and size [mm] with standard deviation per magnification setting. Note that S0-S2 was deployed for approximately 1 h and S3 for ½ hour.

Taxa	Count [ind]				Density [ind/m ³]				Size [mm] with standard deviation			
	S0	S1	S2	S3	S0	S1	S2	S3	S0	S1	S2	S3
Annelida	0	0	7	8	0.00	0.00	8.49	7.96			3.069 ± 1.235	3.292 ± 1.633
Appendicularia	0	7	46	159	0.00	78.48	55.79	158.25		2.064 ± 0.444	2.276 ± 0.260	2.563 ± 0.317
Appendicularia house	0	1	7	867	0.00	11.21	8.49	862.92		2.191 ± 0	2.563 ± 0.483	3.766 ± 0.856
Calanoida	3	0	7	22	422.19	0.00	8.49	21.90	0.706 ± 0.087		1.026 ± 0.360	1.145 ± 0.221
Caridea	0	0	0	3	0.00	0.00	0.00	2.99				2.794 ± 0.261
Chaetognatha	0	0	0	1	0.00	0.00	0.00	1.00				
Cnidaria	1	11	75	80	140.73	123.33	90.96	79.62	0.379 ± 0	1.478 ± 0.327	1.593 ± 0.294	2.205 ± 1.076
Ctenophora	0	1	0	0	0.00	11.21	0.00	0.00		2.059 ± 0		
Cumacea	0	0	9	0	0.00	0.00	10.91	0.00			2.526 ± 0.135	
Echinodermata	0	2	11	36	0.00	22.42	13.34	35.83		1.443 ± 0.087	1.683 ± 0.594	1.540 ± 0.499
Noctiluca	386	827	5033	22,708	54,321.55	9272.35	6103.77	22,601.21	0.715 ± 0.066	0.683 ± 0.078	0.694 ± 0.076	0.965 ± 0.207
Phaeocystis	0	0	0	1280	0.00	0.00	0.00	1273.98				2.768 ± 0.763
Pisces larvae	0	0	1	1	0.00	0.00	1.21	1.00			2.667 ± 0	3.441 ± 0
Σ	390	849	5196	25,165	54,884.46	9519.02	6301.45	25,046.65				

Size was determined by ImageJ length measurements of the particles [mm], with a maximum of 10 measured particles per taxa per magnification. Note that size does not reflect the head-tail length of the organisms but are the longest or widest part of an organism.

4. Discussion

4.1. Tow types

Each of the investigated tow types had their own advantages and limitations, resulting in different possibilities for analyses of the plankton community and abilities to distinguish patterns (Table 6). The Z-shaped pattern was an easy pattern to sail. Despite the fact that the VPR was deployed for 1.5 h, information on different depths was only collected for a relatively small transect. Moreover, the information was collected at three fixed depths, which could lead to the overlooking of important data in the intermittent layers (in case of e.g., stratification). Although the total plankton density was large, the results show that this tow type yielded the largest number of absent taxa. Three of the taxa that were not observed by this particular tow type were species with a benthic lifestyle (Amphipoda, Cumacea and Harpacticoida), illustrating that in this case the water body close to the seafloor was not sampled by the deepest transect of the Z-shaped pattern. However, for the most abundant taxa there were clear vertical distribution patterns because extensive data had been collected at those specific depths. We could therefore say that in case there is sufficient prior knowledge of the marine system or species behavior, and the research question focuses on specific depths (e.g., differences above and below a thermo- or halocline, layer where certain abundant organisms occur), this tow type is adequate. It is also useful to perform quick technical tests because it does not require a dedicated person winching during data collection.

The clover pattern was the most difficult pattern to sail because the current speed, the maximum speed that can be used when deploying the VPR, and the time each loop must have, must be taken into account. Undulating the VPR requires a focused winch operator. This person has to control the VPR's depth continuously, to safeguard the VPR from hitting the seafloor or colliding with the aftdeck of the ship. At all times, the VPR has to stay far enough from the sea surface and the seafloor which changes in depth during deployment. During the transect, various factors such as the sailing direction, sailing speed and current direction relative to the vessel continuously change, making it harder to translate and interpret abiotic parameters linked to currents and tides. The (a)

biotic data covers the whole water column and biological vertical patterns can be distinguished. The Z-pattern however had approximately 30 min of observations on a fixed depth, whereas the clover pattern samples all depths, yet only for a short period. When sampling time is not long enough, it is therefore possible that rare or less abundant taxa are missed, making vertical distribution differences less pronounced. For the reasons stated above, the use of the clover pattern is not recommended for general use nor as a tow type to investigate the influence of the environment on the plankton distribution.

The straight pattern collected data on the whole water column over a long distance. It is an easy pattern to sail and requires a focused winch operator. Compared to the other tow types, this type recorded the highest number of plankton taxa. Vertical distribution patterns were observed for abundant species but, as with the clover pattern, might be harder to detect for rare and less abundant taxa when sampling time is short. Yet a clear difference was observed horizontally on each side of the sandbank. Both horizontally and vertically valuable abiotic data were collected in which gradients and patterns were recognizable. Because the data were collected in one straight line, it is easier to grasp how e.g., currents influence the observations. This tow pattern is suitable for monitoring purposes, studies in a stratified environment or studies interested in plankton distributions.

When comparing these tow types with previous VPR studies, it is noted that most studies undulated the VPR vertically through the water column while remaining almost stationary with the research vessel (Ashjian et al., 2005; Dennett et al., 2002; Jacobsen and Norrbin, 2009; Sainmont et al., 2014). This method yields detailed information on the vertical distribution of species and their interactions with the environment on certain stations but only provides information very locally. An advantage of the VPR is that it can be operated while sailing, allowing it to collect data covering large areas with a high small-scale spatial resolution and allowing it to look into spatial (horizontal and vertical) distribution of plankton. Therefore some studies performed long straight transects (Takahashi et al., 2015; Gislason et al., 2016) or sailed a, as viewed from above, clover-shaped patterns (Möller et al., 2012) or zigzag patterns (Davis et al., 2004) to get more insight into the 3D distribution of plankton. In these previous studies it was often not argued

Table 5

Captured images of various plankton taxa observed with the four magnification settings.

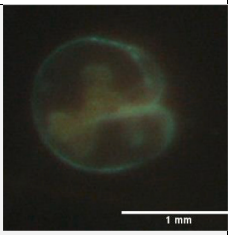

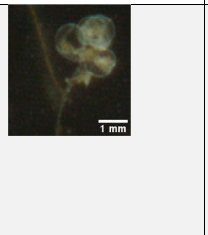
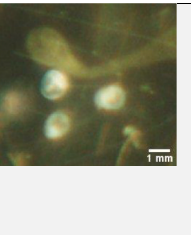
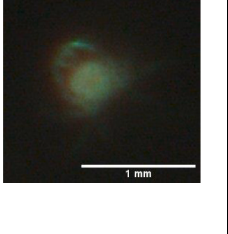
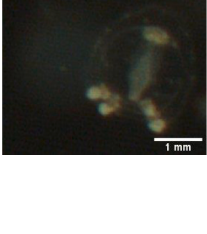
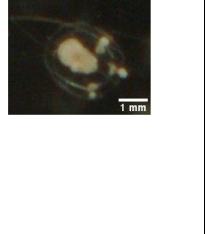
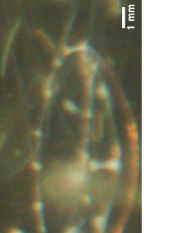
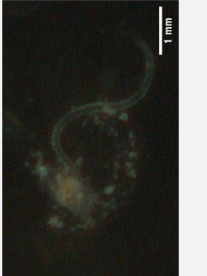

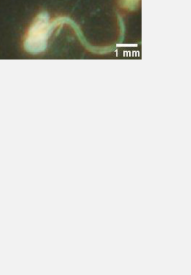
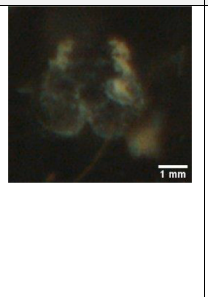
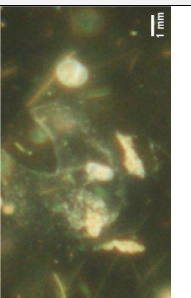
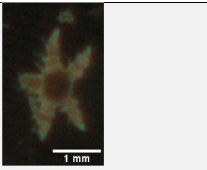
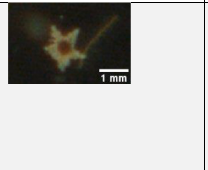

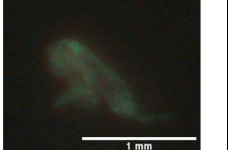
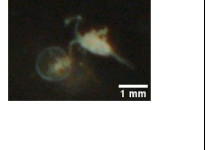
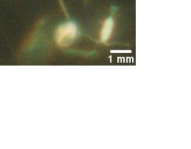
	S0	S1	S2	S3
<i>Noctiluca</i>				
Cnidaria				
Appendicularia	/			
Appendicularia house	/	/		
Echinodermata	/			
Calanoida		/		

Table 6

Comparison of the three tow types: the Z-shaped, clover-shaped and straight pattern.

	Z-shaped	Clover-shaped	Straight
Sailing the pattern	Easy.	Difficult maneuver to make for the captain.	Easy.
Operating the VPR	Easy.	Requires a focused person.	Requires a focused person.
Distance covered	Vessel sailed 10.2 km, but only a \pm 3.4 km trajectory was sampled at three depths.	10.2 km	8.3 km
Total abundance of all plankton	17,576 ind/m ³	16,952 ind/m ³	16,100 ind/m ³
Presence/absence of taxa (relative to the other tow types in this study)	4 taxa absent	2 taxa absent	No taxa absent
Biological patterns	Clear differences in vertical distribution of abundant taxa.	Differences in vertical distribution of abundant taxa.	Differences in vertical distribution of abundant taxa. Large difference in horizontal distribution of abundant taxa between each side of the sandbank.
Abiotic measurements: temperature and turbidity	Vertical differences in water temperature and turbidity observed. Only information on 3 fixed depths.	Vertical differences in water temperature and turbidity observed. Information on the whole water column.	Vertical and horizontal differences in water temperature and turbidity observed. Information on the whole water column.
Recommended application	-Technical tests -Research interest in specific depths -Research in small area	-Research in small area	-In stratified environments -Research interest in horizontal or vertical (e.g., vertical migration) distribution of plankton -Monitoring purposes -General insight in plankton community -Research in large area, covering great distance

why the choice was made for a particular towing technique. When researchers aim to collect 3D data on a broad surface, the straight pattern could also be extended to make a zigzag pattern as seen from above (as in Davis et al., 2004) instead of a straight line, collecting data on depth, length and width.

Things to keep in mind when deploying the VPR, especially during Z-profiles and clover-shaped patterns, are currents and tides. With a semidiurnal regime in our study area (Baeye et al., 2011) the current direction and speed quickly changes. For the Z and clover-shaped pattern, it is necessary to tow in the same area to have information on the same waterbody at different depths. When Z patterns are performed at many depths, it is possible that the currents have supplied a new water mass by the time the entire water column has been traversed. Changes between top and bottom layers may therefore be due to the new water

mass brought in by currents or tides, rather than changes or gradients within the same water body. The same problem applies to the clover pattern as it assumes that the same area around a central point is sampled. If the loops are too large, the area will not be mapped more extensively but will different water masses be mapped. The semidiurnal tidal cycling in the BPNS causes an anti-clockwise veering of the water during the ebb and flood currents (Otto et al., 1990) with current velocities maxima up to 1.66 m/s (Verfaillie, 2008). It cannot be ruled out that the currents had an impact on the data collected within a particular tow type, although we expect that the impact was minimal because no significant abiotic changes could be observed between the loops of the clover pattern. The clear temperature changes observed in the Z-pattern are thus likely related to depth rather than the effect of the currents.

It should be noted that the comparison between the tow types in the field is hard to do in exactly the same water mass. The time between the start of the first and the end of the last tow type covers almost a half tidal cycle (i.e., the transition from ebb till flood), as a result of which the water mass at the start and end point possibly strongly differ. The tow types were performed immediately after each other, to restrict natural variation to a minimum, but this is an unavoidable parameter during field studies.

4.2. Magnification settings

The magnification of the VPR will impact which size range of particles are captured by the VPR. The field of view magnification setting S0 is 8.8 mm by 6.6 mm, which theoretically implies that particles up to 8.8 mm could be photographed. However, we see that this is not the case and that the largest mean size of plankton taxa observed with S0 was 0.715 mm, while the ZooScan and ImageJ measurements indicated that plankton particles of 0.35 till 3.77 mm were present in the water column. The results also show that with a high magnification setting mainly smaller organisms (around 0.4–0.7 mm) are observed while a low magnification setting captures larger particles (around 1.0–3.8 mm), as is represented in Table 7. We expect that the magnification itself is the main reason for this result, rather than the lower encounter chance of e.g., large organisms associated with a smaller sampled volume. Despite the smaller sampling time and thus sampled volume of S3, it still observed larger organisms.

Choosing the most suitable magnification setting is a trade-off between image detail, image size range and encounter chance of particles. When there is a research interest for a specific plankton taxon or size fraction of the plankton community, then this can be the main driver to decide on the used magnification setting. When there is an interest in larger organisms (>2–3 mm) such as cnidarians the lowest magnification setting is the most suitable due to its large field of view. Pan et al. (2018) decided to use the lowest magnification setting due to the dominance of macrozooplankton with copepods and gelatinous species in their study area. Vice versa, Möller et al. (2012) used the largest magnification due to the small particle and plankton sizes in the sampling area. This magnification was deemed suitable for imaging small sized adult calanoid copepod species (e.g., *Acartia* spp., *Temora longicornis* and *Pseudocalanus acuspes*), known to dominate the mesozooplankton community in their study area. Beside plankton taxa and abundance, there is also additional information to be obtained from the image such as stomach content, presence of an egg sac, length of appendages, colony formation, foraging on detritus, ... When a study focuses on a particular feature of an organism, a high magnification setting can give the most detailed image with the highest resolution possible where features are the clearest visible. If the researcher is however interested in larger aggregates of e.g., colony forming organisms or organisms feeding on detritus, then a lower magnification might be more suitable due to the larger field of view where large aggregates can be photographed. When research is dealing with a less common organism, a low magnification setting could enlarge the encounter chance with it because of the large field of view and the larger imaged volume. When

Table 7
Comparison of the four magnification settings.

	S0	S1	S2	S3
Field of view	8.8 × 6.6 mm	20.8 × 15.2 mm	33.8 × 25.5 mm	46.5 × 34.5 mm
Imaged volume per frame of the campaign in June 2020	2.021 mL	23.391 mL	192.657 mL	285.758 mL
Particles on photo	-Single particle on ROI	-Multiple particles on ROI possible -Possibility to see the interaction with environment (e.g., organisms feeding on detritus)	-Multiple particles on ROI possible -Possibility to see the interaction with environment (e.g., organisms feeding on detritus)	-Multiple particles on ROI possible -Possibility to see the interaction with environment (e.g., organisms feeding on detritus)
Image detail	Most detailed (e.g., stomach content of <i>Noctiluca</i> visible)			Least detailed (e.g., not possible to distinguish certain characteristics of small organisms)
Plankton size of captured images	Approximately 0.4 to 0.7 mm	Approximately 0.7 to 2.2 mm	Approximately 0.7 to 3.1 mm	Approximately 1.0 to 3.8 mm (e.g., larger gelatinous species or colony-forming species)

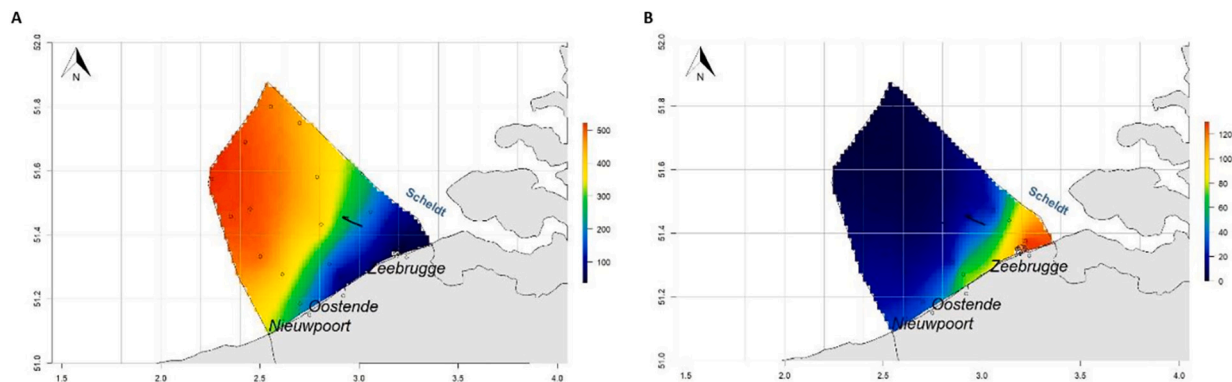


Fig. 5. Interpolated map of (A) the Secchi depth [cm] and (B) SPM concentrations [mg/L] in June 2020. The VPR trajectory is represented in black.

there is a general interest in the whole plankton community, then the results indicate that S1 is a good middle ground to avoid that only too small or too large images are missed, without losing too much image detail and still being able to observe interactions with the environment (e.g., particles feeding on detritus). If, however, the VPR would be used in addition to traditional net sampling techniques, then it might be valuable to use setting S3. The VPR could then, in addition to the regular observations, detect organisms (like large gelatinous species) that are otherwise missed or destroyed with net sampling techniques (Remsen et al., 2004; Dennett et al., 2002). It also should be noted that despite the various magnifications, the VPR provides information about organisms only in a coarse taxonomic resolution and not down to species level, even with the highest magnification (Davis et al., 2004).

4.3. Turbidity

In situ optical sampling methods cannot be used in every water type. In general, the VPR is towed in clear, low turbidity waters such as Atlantic or Arctic environments (Dennett et al., 2002; Jacobsen and Norrbin, 2009; Sainmont et al., 2014). These open water systems are much different from the turbid coastal area in this study. The results show that high turbidity values over 6.2 NTU hamper the efficient use of the VPR, illustrating the importance of turbidity on the use of the VPR. As turbidity rises, images become more blurry until no more images are captured at all. The VPR makes use of dark field imaging, meaning that the light sent out by the stroboscope is diffracted by particles of interest and subsequently captured by the camera lens. When turbidity is high, other particles in the background, whether these are detritus, phytoplankton blooms or other small particulate matter suspended in the water column, can as well diffract light, thereby highlighting the background and making the particle of interest less visible and less contrasting with the background. This observation is also noted by Davis

et al. (1992): VPR images from in situ field experiments had a slightly lower contrast compared to laboratory images due to the fairly turbid conditions in the field. When turbidity in the BPNS exceeds 10.2 NTU, no more images are captured: the AutoDeck software that automatically extracts and saves ROIs from the raw VPR images is no longer able to distinguish the particles from the background. For the deployment of other optical imaging devices, turbidity should also be considered as a potential limiting factor.

In the coastal area there is a clear gradient with high turbidity values close to the shore towards low turbidity values further away from the coast. During a transect towards the coast with the same AutoDeck settings, gradually fewer images would be taken when the coastline is approached. Less plankton will be captured at the end of the transect even if the plankton densities were the same in the whole study area, resulting in an underestimation of the plankton community at the end of the transect. When deploying the VPR, it is therefore important to sail in areas with sufficient clear water in terms of turbidity (< 6.2 NTU) and to avoid ending a transect in turbid zones.

Due to the turbidity restrictions on the use of the VPR, coastal areas or areas with a too high turbidity, will require other techniques to sample the plankton community. Plankton net samples can offer a solution and optical methods where the lens and light source are closer together (e.g., CPICS (Coastal Ocean Vision, Inc.; Gallagher, 2016)) could enlarge the sampling range to a limited extent.

Although a high turbidity restricts the capture of images, it does not affect the turbidity and CTD sensor. Additionally there is the possibility, based on own experience, to mount extra sensors such as a LISST-200X (Sequoia Scientific, Inc.) on the back of the VPR causing the VPR to also be a suitable device to get more information on the composition or grains size of the entirety of suspended particles that cause turbidity.

4.4. Case study of applicability in the BPNS

In addition to turbidity and current dynamics, the VPR's effectiveness and usage is further restricted by three main factors: depth of the water column, tides and wave height. A safety distance of e.g., 3 m from the seabed and surface is advised to avoid a collision of the VPR with the seabed or rear deck. In shallow areas or during low tide, this leaves little room for the VPR to undulate through the water column. Moreover, wave heights above 1.5 m impede VPR deployment in a safe way for machine and crew.

The BPNS is an intensively used area and shipping routes, ship wrecks and windmill parks impose restrictions on where the VPR can be used (Supplementary Material Fig. 1). The North Sea area contains some of the busiest shipping routes in the world and due to the shallow depths, vessel traffic is confined within narrow navigation channels (Volckaert, 2006). Busy areas within the route system can be transversed with the research vessel but sailing back and forth should be avoided to limit the possibilities of collision. Additionally, permissions are needed to enter the windmill parks and a safe distance to the windmill pillars has to be guaranteed. Also seafloor obstructions such as shipwrecks must be treated with caution as it is not always possible to estimate how high these protrude above the seabed.

5. Conclusions

The VPR has proven to be a valuable instrument that is flexible to the local conditions and can be adapted to the research objective. It can be particularly useful in studies where it is essential to look at the vertical distribution of organisms through the water column or where high spatial and temporal resolution is necessary, which cannot be achieved with traditional net sampling methods (Remsen et al., 2004; Dennett et al., 2002). Our study shows that depending on the towing procedure, the information to be extracted from the collected data and the ability to distinguish (a)biotic patterns differs. Whereas a Z-shaped and a clover tow type are suitable for detailed characterization of the plankton community of a limited geographical area, a straight tow type is more suitable for plankton studies over a larger area, with the possibility to more easily interpret the influence of environmental factors on the plankton community, compared to the other tow types. The size of the plankton taxa under study should be the main determinant when choosing the magnification setting, with high magnifications being more suitable for smaller organisms (0.3–0.7 mm) and vice versa (1.0–3.8 mm). If there is no specific focus on a certain taxon, then an intermediate magnification setting S1 is suggested as it avoids that only too large or only too small particles are excluded, while still having sufficient image detail. This study also highlighted some restrictions considering the employability and working range of the VPR. It shows that in areas with a high turbidity, such as coastal systems, the VPR no longer functions optimally, inhibiting the collection of useable image data. The VPR, and with extension other optical methods, therefore needs to be deployed in sufficiently clear waters, with a turbidity threshold of 6.2 NTU for the type of VPR studied here.

Author contributions

AO: processing of the data, analyses, and writing. JM: processing of the data, project supervision, and reviewing. MV: project supervision and reviewing. RD: technical support, reviewing. MDT: reviewing. KD: project supervision, reviewing. All authors contributed to the article and approved the submitted version.

Funding

This work was supported by the Flanders Marine Institute (VLIZ). It makes use of data and infrastructure provided by the VLIZ and funded by the Research Foundation—Flanders (FWO) as part of the Belgian

contribution to the LifeWatch European Research Infrastructure [grant numbers I000819N-LIFEWATCH and I002021N-LIFEWATCH].

Declaration of Competing Interest

The authors declare that they have no known competing financial interests or personal relationships that could have appeared to influence the work reported in this paper.

Data availability

Data will be made available on request.

Acknowledgements

We wish to thank the crew of the RV Simon Stevin, as well as the students and interns who have been processing the zooplankton samples with the ZooScan and Video Plankton Recorder over the years.

Appendix A. Supplementary data

Supplementary data to this article can be found online at <https://doi.org/10.1016/j.seares.2022.102257>.

References

- Ashjian, C.J., Davis, C.S., Gallagher, S.M., Alatalo, P., 2001. Distribution of plankton, particles, and hydrographic features across Georges Bank described using the video plankton recorder. *Deep-Sea Res. II Top. Stud. Oceanogr.* 48 (1–3), 245–282. [https://doi.org/10.1016/S0967-0645\(00\)00121-1](https://doi.org/10.1016/S0967-0645(00)00121-1).
- Ashjian, C.J., Davis, C.S., Gallagher, S.M., Alatalo, P., 2005. Characterization of the zooplankton community, size composition, and distribution in relation to hydrography in the Japan/East Sea. *Deep Sea Research Part II: Topical Studies in Oceanography* 52 (11–13), 1363–1392. <https://doi.org/10.21236/ada630084>.
- Baeye, M., Fettweis, M., Voulgaris, G., Van Lancker, V., 2011. Sediment mobility in response to tidal and wind-driven flows along the Belgian inner shelf, southern North Sea. *Ocean Dyn.* 61 (5), 611–622. <https://doi.org/10.1007/s10236-010-0370-7>.
- Castellani, C., Edwards, M. (Eds.), 2017. *Marine Plankton: A Practical Guide to Ecology, Methodology, and Taxonomy*. Oxford University Press. <https://doi.org/10.1093/oso/9780199233267.001.0001>.
- Chivers, W.J., Walne, A.W., Hays, G.C., 2017. Mismatch between marine plankton range movements and the velocity of climate change. *Nat. Commun.* 8 (1) <https://doi.org/10.1038/ncomms14434>.
- Davis, C.S., Gallagher, S.M., Berman, M.S., Haury, L.R., Strickler, J.R., 1992. The Video Plankton Recorder (VPR): Design and initial results. *Arch. Hydrobiol. Beih.* 36, 67–81.
- Davis, C., Hu, Q., Gallagher, S., Tang, X., Ashjian, C., 2004. Real-time observation of taxa-specific plankton distributions: an optical sampling method. *Mar. Ecol. Prog. Ser.* 284, 77–96. <https://doi.org/10.3354/meps284077>.
- De Galan, S., Elskens, M., Goeyens, L., Pollentier, A., Brion, N., Baeyens, W., 2004. Spatial and temporal trends in nutrient concentrations in the Belgian continental area of the North Sea during the period 1993–2000. *Estuar. Coast. Shelf Sci.* 61 (3), 517–528. <https://doi.org/10.1016/j.ecss.2004.06.015>.
- De Lafontaine, Y., Leggett, W.C., 1989. Changes in size and weight of hydromedusae during formalin preservation. *Bull. Mar. Sci.* 44 (3), 1129–1137.
- Dennett, M.R., Caron, D.A., Michaels, A.F., Gallagher, S.M., Davis, C.S., 2002. Video plankton recorder reveals high abundances of colonial Radiolaria in surface waters of the central North Pacific. *J. Plankton Res.* 24 (8), 797–805. <https://doi.org/10.1093/plankt/24.8.797>.
- Fettweis, M., Nechad, B., Van den Eynde, D., 2007. An estimate of the suspended particulate matter (SPM) transport in the southern North Sea using SeaWiFS images, in situ measurements and numerical model results. *Cont. Shelf Res.* 27 (10–11), 1568–1583. <https://doi.org/10.1016/j.csr.2007.01.017>.
- Flanders Marine Institute (VLIZ), 2019. *LifeWatch Observatory Data: Nutrient, Pigment, Suspended Matter and Secchi Measurements in the Belgian Part of the North Sea*. Flanders Marine Institute (VLIZ), Oostende.
- Gallagher, S.M., 2016. The continuous plankton imaging and classification sensor (CPICS): a sensor for quantifying Mesoplankton biodiversity and community structure. *Am. Geophys. Union* 2016, 52A–57A.
- Gallienne, C., Robins, D., Woodd-Walker, R., 2001. Abundance, distribution and size structure of zooplankton along a 20° west meridional transect of the Northeast Atlantic Ocean in July. *Deep-Sea Res. II Top. Stud. Oceanogr.* 48 (4–5), 925–949. [https://doi.org/10.1016/S0967-0645\(00\)00114-4](https://doi.org/10.1016/S0967-0645(00)00114-4).
- Gislason, A., Logemann, K., Marteinsdottir, G., 2016. The cross-shore distribution of plankton and particles southwest of Iceland observed with a video plankton recorder. *Cont. Shelf Res.* 123, 50–60. <https://doi.org/10.1016/j.csr.2016.04.004>.

- Gorsky, G., Ohman, M.D., Picheral, M., Gasparini, S., Stemmann, L., Romagnan, J.-B., Prejer, F., 2010. Digital zooplankton image analysis using the ZooScan integrated system. *J. Plankton Res.* 32 (3), 285–303. <https://doi.org/10.1093/plankt/fbp124>.
- Grosjean, P., Picheral, M., Warembourg, C., Gorsky, G., 2004. Enumeration, measurement, and identification of net zooplankton samples using the ZOOSCAN digital imaging system. *ICES J. Mar. Sci.* 61 (4), 518–525. <https://doi.org/10.1016/j.jicesjms.2004.03.012>.
- Jacobsen, H., Norrbin, M., 2009. Fine-scale layer of hydromedusae is revealed by video plankton recorder (VPR) in a semi-enclosed bay in northern Norway. *Mar. Ecol. Prog. Ser.* 380, 129–135. <https://doi.org/10.3354/meps07954>.
- Mackas, D.L., Greve, W., Edwards, M., Chiba, S., Tadokoro, K., Eloire, D., Peluso, T., 2012. Changing zooplankton seasonality in a changing ocean: comparing time series of zooplankton phenology. *Prog. Oceanogr.* 97–100, 31–62. <https://doi.org/10.1016/j.pocean.2011.11.005>.
- Möller, K., St John, M., Temming, A., Floeter, J., Sell, A., Herrmann, J., Möllmann, C., 2012. Marine snow, zooplankton and thin layers: indications of a trophic link from small-scale sampling with the video plankton recorder. *Mar. Ecol. Prog. Ser.* 468, 57–69. <https://doi.org/10.3354/meps09984>.
- Mortelmans, J., Deneudt, K., Cattijse, A., Beauchard, O., Daveloose, I., Vyverman, W., Mees, J., 2019. Nutrient, pigment, suspended matter and turbidity measurements in the Belgian part of the North Sea. *Sci. Data* 6 (1). <https://doi.org/10.1038/s41597-019-0032-7>.
- Nielsen, T., Løkkegaard, B., Richardson, K., Bo Pedersen, R., Hansen, L., 1993. Structure of plankton communities in the Dogger Bank area (North Sea) during a stratified situation. *Mar. Ecol. Prog. Ser.* 95, 115–131. <https://doi.org/10.3354/meps095115>.
- Nihoul, J.C.J., Rondal, F.C., Peters, J.J., Sterling, A., 1978. Hydrodynamics of the Scheldt estuary. *Elsevier Oceanogr. Ser.* 27–53. [https://doi.org/10.1016/s0422-9894\(08\)71270-4](https://doi.org/10.1016/s0422-9894(08)71270-4).
- Nishikawa, J., Terazaki, M., 1996. Tissue shrinkage of two gelatinous zooplankton, *Thalia democratica* and *Doliolletta gegenbauri* (Tunicata: Thaliacea) in preservative. *Bull. Plankton Soc. Jpn.* 43 (1), 1–7.
- Otto, L., Zimmerman, J.T.F., Furnes, G.K., Mork, M., Sætre, R., Becker, G., 1990. *Neth. J. Sea Res.* 26 (2–4), 161–238.
- Pan, J., Cheng, F., Yu, F., 2018. The Diel Vertical Migration of Zooplankton in the Hypoxia Area Observed by Video Plankton Recorder.
- Remsen, A., Hopkins, T.L., Samson, S., 2004. What you see is not what you catch: a comparison of concurrently collected net, optical plankton counter, and shadowed image particle profiling evaluation recorder data from the Northeast Gulf of Mexico. *Deep-Sea Res. I Oceanogr. Res. Pap.* 51 (1), 129–151. <https://doi.org/10.1016/j.dsr.2003.09.008>.
- RStudio Team, 2020. RStudio: Integrated Development for R. RStudio, PBC, Boston, MA. <http://www.rstudio.com/>.
- Sainmont, J., Gislason, A., Heuschele, J., Webster, C.N., Sylvander, P., Wang, M., Varpe, Ø., 2014. Inter- and intra-specific diurnal habitat selection of zooplankton during the spring bloom observed by video plankton recorder. *Mar. Biol.* 161 (8), 1931–1941. <https://doi.org/10.1007/s00227-014-2475-x>.
- Seascan, Inc, 2014. Real Time Video Plankton Recorder Owner's Manual. Author, Falmouth, WA.
- Steinberg, D.K., Landry, M.R., 2017. Zooplankton and the ocean carbon cycle. *Annu. Rev. Mar. Sci.* 9, 413–444.
- Studio 3T Team, 2022. Studio 3T: The Professional Client, IDE & GUI for MongoDB. <https://studio3t.com>.
- Takahashi, K., Ichikawa, T., Fukugama, C., Yamane, M., Kakehi, S., Okazaki, Y., Furuya, K., 2015. In situ observations of a doliolid bloom in a warm water filament using a video plankton recorder: bloom development, fate, and effect on biogeochemical cycles and planktonic food webs. *Limnol. Oceanogr.* 60 (5), 1763–1780. <https://doi.org/10.1002/lno.10133>.
- Thibault-Botha, Delphine, Bowen, Terra, 2004. Impact of formalin preservation on *Pleurobrachia bachei* (Ctenophora). *J. Exp. Mar. Biol. Ecol.* 303 (1), 11–17.
- Vanaverbeke, J., Gheskiere, T., Vincx, M., 2000. The Meiobenthos of subtidal sandbanks on the Belgian continental shelf (southern bight of the North Sea). *Estuar. Coast. Shelf Sci.* 51 (5), 637–649. <https://doi.org/10.1006/ecss.2000.0703>.
- Verfaillie, E., 2008. PhD Thesis. Ontwikkeling en validatie van een ruimtelijke verspreidingsmodellen van mariene habitats, ter ondersteuning van het ecologisch waarden van de zeebodem = Development and validation of spatial distribution models of marine habitats, in support of the ecological valuation of the seabed. Instituut voor de Aanmoediging van Innovatie door Wetenschap en Technologie in Vlaanderen/RCMG/Universiteit Gent: Brussel, p. 207 pp.
- Volckaert, A.M., et al., 2006. Marine Incidents Management Cluster (MIMAC): Research in the framework of the BELSPO Supporting Actions-SPSDII. MIMAC 2006: International Conference on Marine Incidents Management, Brugge, Belgium, 19-20 October 2006. VLIZ Special Publication.